

Research Article

Photocatalytic Degradation of 2-Chlorophenol Using Ag-Doped TiO₂ Nanofibers and a Near-UV Light-Emitting Diode System

Ju-Young Park^{1,2} and In-Hwa Lee¹

¹ Department of Environmental Engineering, Chosun University, Gwangju 501-759, Republic of Korea

² Center for Novel States of Complex Materials Research, Department of Physics and Astronomy, Seoul National University, Seoul 151-747, Republic of Korea

Correspondence should be addressed to In-Hwa Lee; ihlee@chosun.ac.kr

Received 4 October 2013; Accepted 11 December 2013; Published 8 January 2014

Academic Editor: Ranjit T. Koodali

Copyright © 2014 J.-Y. Park and I.-H. Lee. This is an open access article distributed under the Creative Commons Attribution License, which permits unrestricted use, distribution, and reproduction in any medium, provided the original work is properly cited.

This report investigated the photocatalytic degradation of 2-chlorophenol using TiO₂ nanofibers and Ag-doped TiO₂ nanofibers, synthesized using the sol-gel and electrospinning techniques, and an ultraviolet light-emitting diode (UV-LED) system as a UV light source. The crystallite size of the Ag-doped TiO₂ nanofibers was smaller than that of the TiO₂ nanofibers, because silver retrained phase transformation not only controls the phase transformation but also inhibits the growth of anatase crystallites. The activation energies for the grain growth of the TiO₂ nanofibers and the Ag-doped TiO₂ nanofibers were estimated to be 20.84 and 27.01 kJ/mol, respectively. The photocatalytic degradation rate followed a pseudo-first-order equation. The rate constants (*k*) of the TiO₂ nanofibers and the Ag-doped TiO₂ nanofibers were 0.056 and 0.144 min⁻¹, respectively.

1. Introduction

TiO₂ is the most widely used photocatalyst owing to its photostability, nontoxicity, low cost, and insolubility in water under most environmental conditions [1]. Excitation of TiO₂ generates highly reactive electron-hole pairs that subsequently produce highly potent radicals (such as [•]OH and O₂^{•-}) that oxidize organic and inorganic pollutants. However, the optimal design of the reactor and the various operational conditions are major concerns in the development and potential applications of photocatalytic processes. Virtually all previous work on photocatalytic degradation with respect to the removal of pollutants from wastewater has been carried out using broad spectral radiation sources, such as UV lamps, and TiO₂ as the photocatalyst. The traditional UV source is a mercury vapor high-pressure lamp, which is also a source of gas discharge [2, 3]. The mercury used in this UV lamp is specified as a hazardous air pollutant by the U.S. Environmental Protection Agency and can damage the brain and kidneys. Ultraviolet light-emitting diodes (UV-LEDs) are a new, safer, and energy efficient alternative to traditional

gas discharge sources. LEDs are a directional light source, in which the maximum emitted power is in the direction perpendicular to the emitting surface. A typical lifetime of 100,000 h is another advantage of UV-LEDs, whereas the lifetime of gas discharge sources is approximately 1000 h. The electrospinning technique has been recognized as a versatile and effective method for the preparation of nanofibers with small diameters and high surface-to-volume ratios [4–7], and the fabrication of TiO₂ nanofibers by electrospinning was first reported in 2003 [8]. Some researchers have already prepared pure inorganic fibers comprised of TiO₂ [9–11]. Based on these previous reports, TiO₂ fibers were fabricated from a mixture of titanium isopropoxide (TiIP) and a polymer using electrospinning techniques. After thermal treatment, TiO₂ (anatase and/or rutile phase) fibers were obtained. Bender et al. [12], Alves et al. [13], and Ding et al. [14] studied the electrospun TiO₂ nanofibers as a photocatalyst to be applied to the degradation of dye pollutants. However, there has been very little research on photocatalytic degradation using metal-doped (Ag, Pd, and Pt) TiO₂ nanofibers. Some metal materials, such as Ag, Pd, and Pt, supported on

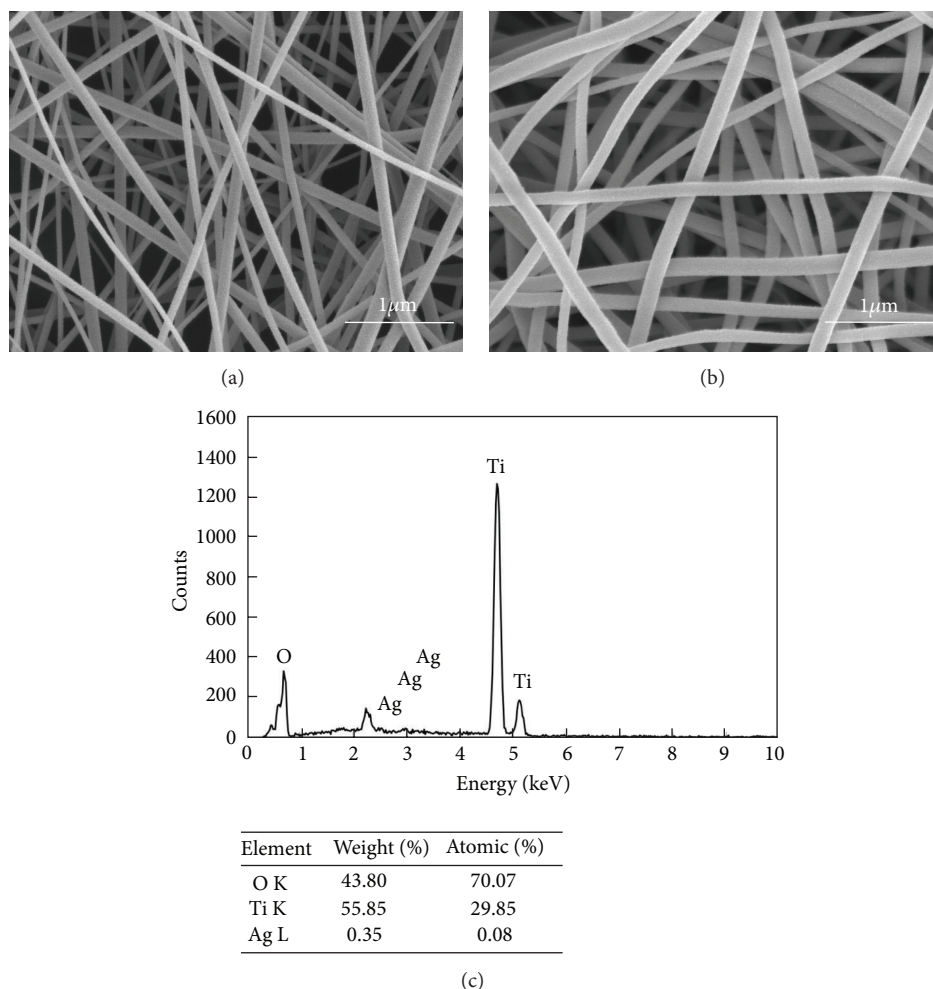


FIGURE 1: FE-SEM images of (a) TiO_2 nanofibers and (b) Ag-doped TiO_2 nanofibers. (c) EDX spectrum of Ag-doped TiO_2 nanofibers.

the TiO_2 surface can greatly accelerate the decomposition rate of organic compound by effectively consuming the photoproduced electrons in the reduction of oxygen, thereby reducing the recombination of electrons (e^-) and holes (h^+) [15–18].

Recently, some researchers have demonstrated the photocatalytic degradation of organic materials using the TiO_2 and UV-LED system [19–21]. The TiO_2 nanofibers photocatalyst is illuminated by the near-UV-LED light source in order to activate its band gap energy and to produce subsequently electron-hole pairs that act as oxidizing and reducing agents.

In this work, Ag-doped TiO_2 nanofibers were prepared using the electrospinning method in order to prevent recombination, which causes the relatively low photocatalytic efficiency. TiO_2 presents the relatively high electron-hole recombination rate which is detrimental to its photoactivity. In this sense, Ag-doped TiO_2 could make a double effect: (1) Firstly, it could reduce the band gap energy, thus shifting the adsorption; (2) secondly, Ag could provoke a decrease in electron-hole recombination rate, acting as electron traps [18]. The photocatalyst samples (TiO_2 nanofibers and Ag-doped TiO_2 nanofibers) were characterized using field-emission scanning electron microscopy (FE-SEM), X-ray

diffraction (XRD), and Brunauer-Emmett-Teller (BET) surface area. The activation energy for the grain growth of the TiO_2 nanofibers was calculated by the Arrhenius equation, based on the XRD results. The photocatalysts were evaluated for the photodecomposition of 2-chlorophenol under the UV-LED system.

2. Experimental

TiO_2 nanofibers and Ag-doped TiO_2 nanofibers were fabricated using the method described by Park et al. [7]. Electrospun nanofibers were prepared using TiP and polyvinylpyrrolidone (PVP) as precursors. 6 mL of TiP was first mixed with 12 mL of acetic acid and 12 mL of ethanol. After 60 min, this solution was added to 30 g of ethanol, which contained 10 wt% PVP and 1.986 mL of 0.5 N AgNO_3 (5% of the molar amount of TiP), followed by magnetic stirring for 24 h. The mixture was immediately loaded into a glass syringe equipped with a 21 G stainless steel needle, and the needle was then connected to a high voltage supply (DC power supply PS/ER 50R06 DM22, Glassman High Voltage Inc., USA). A voltage of 20 kV was applied between the needle

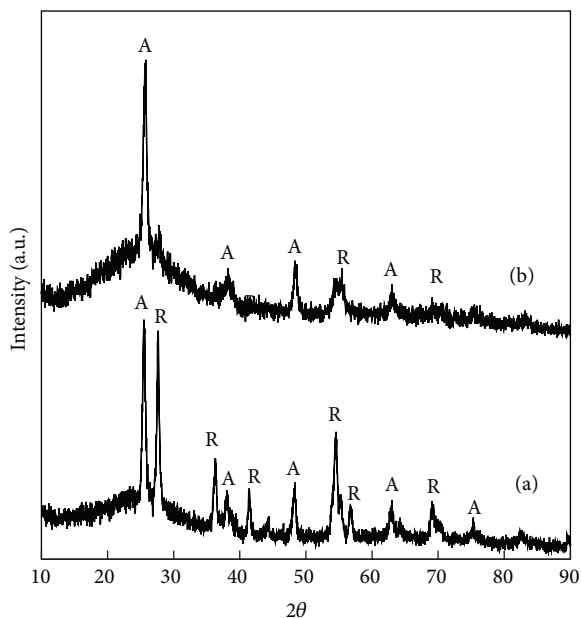


FIGURE 2: XRD patterns of (a) TiO₂ nanofibers and (b) Ag-doped TiO₂ nanofibers.

and the collector, and the distance between the needle and the target was 15 cm. The flow rate was maintained at 50 $\mu\text{L}/\text{min}$ using a syringe.

The prepared electrospun TiP/PVP nanofibers were calcined at 500°C. The morphology of the electrospun TiO₂ nanofibers was observed using FE-SEM (Hitachi, S-4800) with the energy dispersive X-ray (EDX). XRD patterns were recorded using a Philips (X'Pert PR O MPO) diffractometer (Cu K α radiation) at a scanning rate of 0.01°/sec in the 2 θ range of 10° to 90°.

The photo-reactor consists of a planar cell comprised entirely of SS 316 L glass. The planar reactor contained two hollow fillisters that were 205 mm long and 45 mm wide at the top and bottom fixtures, respectively. The UV-LED system, which was used as the UV light source, consisted of a 3 \times 11 array of UV-LEDs (3.3 V, 8 mW, and 365 nm). The 2-chlorophenol (99.9% trace metal basis, Aldrich) was analytical grade, and deionized water was used in all decomposition experiments. The concentrations of the 2-chlorophenol aqueous solutions were analyzed by HPLC (Sykam S210) with an ODS C18 column (150 mm \times 4.6 mm). The eluent was 65% acetonitrile, the flow rate was 1 mL/min, and the absorbance was monitored at 280 nm.

3. Results and Discussion

Figures 1 and 2 show FE-SEM images and XRD patterns, respectively, of the TiO₂ nanofibers and the Ag-doped TiO₂ nanofibers, at a calcination temperature of 500°C. After calcination of the TiP/PVP composite nanofibers, the TiO₂ nanofibers were fabricated by removing the PVP during calcination. TiO₂ nanofibers (Figure 1(a)) and Ag-doped TiO₂ nanofibers (Figure 1(b)) with a diameter of 100 to 150 nm were obtained after calcination at 500°C. Figure 1(c) showed

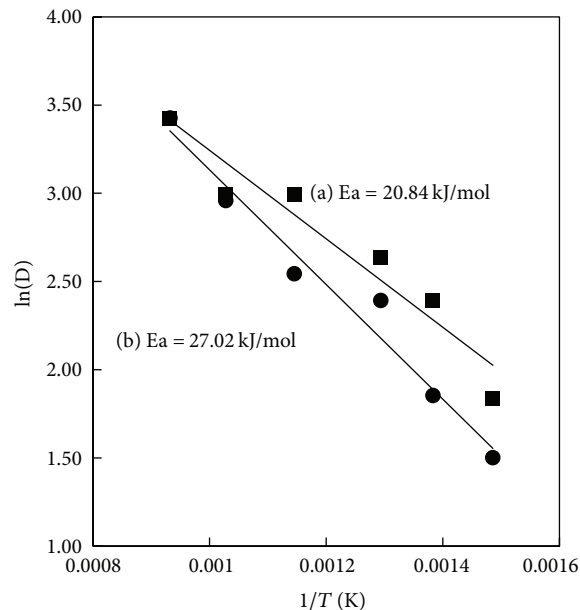


FIGURE 3: Plot of $\ln(D)$ versus $1/T$. The slope provides information about the activation energy for the grain growth of (a) TiO₂ nanofibers and (b) Ag-doped TiO₂ nanofibers.

EDX spectrum at a calcination temperature of 500°C. An Ag doping amount of 0.35 wt.% was estimated from the EDX analysis. According to Park et al. [7], the Ag controlled the phase transformation temperature of the TiO₂ nanofibers. At the Bragg angle (2 θ) of 25.2°, the anatase ratio of the corresponding plane (101) (extracted from XRD pattern) was calculated from the Spurr equation against corresponding plane (101) [22]. TiO₂ nanofibers were observed in both the 46% anatase phase and the 54% rutile phase, and the Ag-doped TiO₂ nanofibers were only observed in the anatase phase.

The grain growth is a thermal activation process, satisfying the well-known Arrhenius equation:

$$D = A \exp\left(\frac{-E_a}{RT}\right), \quad (1)$$

where D is the average grain size, A is preexponential factor, E_a is the activation energy for the atomic diffusion near the grain boundary, R is the gas constant, and T is temperature in Kelvin. Figure 3 shows the plot of $\ln(D)$ as a function of $1/T$ in Kelvin. The activation energy for the grain growth of TiO₂ nanofibers was estimated to be 20.84 kJ/mol from the slope of $\ln(D)$ versus $1/T$, which is lower than the 27.02 kJ/mol value of the Ag-doped TiO₂ nanofibers. The lower activation energy for the growth of nanograins is a result of the chemical potential of the atoms in the nanosize grains being much higher, which leads to more active growth.

Figure 4 shows nitrogen-adsorption measurements of the sample. The Brunauer-Emmett-Teller (BET) surface area of TiO₂ nanofibers and Ag-doped TiO₂ nanofibers was 215.2 and 219.9 m²/g, respectively. The pore volume and pore size of the sample were determined using the DFT method. For the TiO₂ nanofibers and the Ag-doped TiO₂ nanofibers,

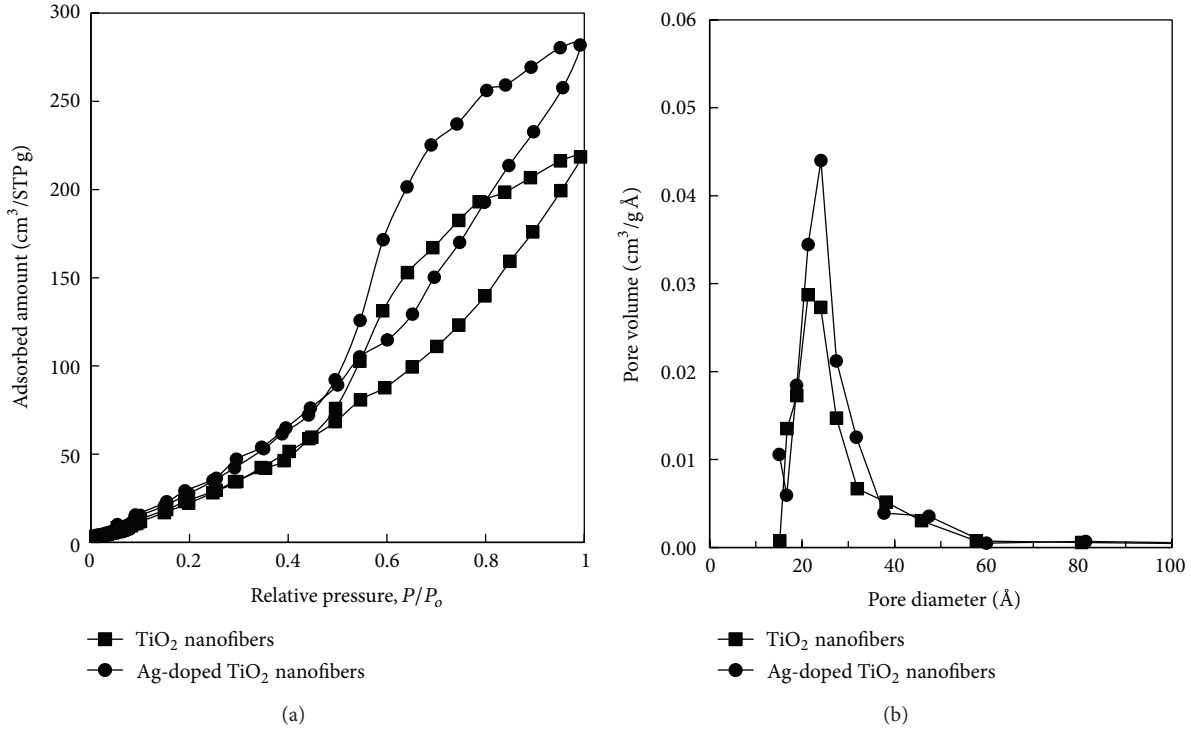


FIGURE 4: Nitrogen adsorption-desorption isotherms and the calculated pore-size distribution.

the pore volumes were 0.136 and 0.410 cm³/g and the pore sizes were 45.40 and 13.85 Å, respectively.

Figure 5 shows the changes in 2-chlorophenol concentration with respect to irradiation time during the UV-LED process. In the case of Ag-doped TiO₂ nanofibers, photodegradation of 2-chlorophenol was increased, which may have been attributed to the following four reasons. (1) Appropriate amount of the doped and deposited Ag species on the surface layer of TiO₂ nanofibers effectively captured the photoinduced electrons and holes. (2) Photoinduced electrons were quickly transferred to the oxygen adsorbed on the surface of TiO₂ nanofibers. (3) The amount of the surface hydroxyl was increased. (4) The response range to light was expanded to the visible region [15]. These advantages of the Ag-doped TiO₂ nanofibers remarkably improved its photocatalytic performance.

We calculated the kinetic constant using a pseudo-first-order equation (2) and a simplified version of the Lagergren equation (3). Based on the adsorption capacity, Lagergren [20] proposed a rate equation for the sorption of a solute from a liquid solution. The Lagergren equation is the most widely used rate equation in liquid-phase sorption processes, and this kinetic model is expressed as

$$\frac{dq_t}{dt} = k_1 (q_e - q_t). \quad (2)$$

Integrating the above equation for the boundary conditions $t = 0$ to $t = t$ and $q_e = q_t$ yields

$$\ln(q_e - q_t) = \ln(q_e - k_1 t). \quad (3)$$

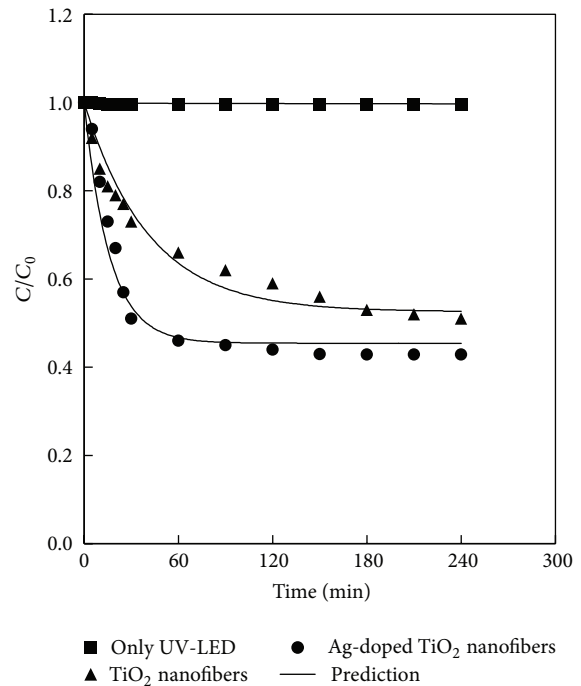


FIGURE 5: Photocatalytic degradation of 2-chlorophenol with the UV-LED system.

The kinetic constant k_1 (min⁻¹) can be determined by plotting $\ln(q_e - q_t)$ against t or $\ln(q_e - q_t)/q_e$ versus t . It is important to note that the correlation coefficients (R^2) of the pseudo-first-order model for the linear plots

TABLE 1: First-order rate constants of the photocatalytic degradation of 2-chlorophenol.

Sample name	Rate constant k (min^{-1})
TiO ₂ nanofibers	0.056
Ag-doped TiO ₂ nanofibers	0.144

of TiO₂ nanofibers are very close to 1. This result implies that the photocatalytic degradation kinetics can be successfully described by this model. The values of the rate constant (k) are listed in Table 1. The rate constants (k) of the TiO₂ nanofibers and the Ag-doped TiO₂ nanofibers were 0.056 and 1.144 min^{-1} , respectively.

4. Conclusions

TiO₂ nanofibers and Ag-doped TiO₂ nanofibers were fabricated by applying the sol-gel and electrospinning techniques. TiO₂ nanofibers and Ag-doped TiO₂ nanofibers were applied as a photocatalyst system with UV-LEDs in order to measure the photocatalytic degradation of 2-chlorophenol. The crystallite size of the Ag-doped TiO₂ nanofibers was smaller than that of the TiO₂ nanofibers, because silver is restrained in this phase transformation. The activation energies for the grain growth of the TiO₂ nanofibers and the Ag-doped TiO₂ nanofibers were 20.48 and 27.02 kJ/mol, respectively. These photocatalysts were evaluated based on the photodecomposition of methylene blue under UV-LEDs. The photocatalytic degradation rate followed a pseudo-first-order equation. The rate constants (k) of the TiO₂ nanofibers and Ag-doped TiO₂ nanofibers were 0.056 and 0.144 min^{-1} , respectively.

Conflict of Interests

The authors declare that there is no conflict of interests regarding the publication of this paper.

Acknowledgments

This work was supported by research fund from Chosun University, 2011. This work was supported by the Human Resources Development Program (no. 20134010200560) of the Korea Institute of Energy Technology Evaluation and Planning (KETEP) grant funded by the Korean Government Ministry of Trade, Industry, and Energy.

References

- [1] D. Li and Y. Xia, "Fabrication of titania nanofibers by electrospinning," *Nano Letters*, vol. 3, no. 4, pp. 555–560, 2003.
- [2] P. Viswanathamurthi, N. Bhattarai, C. K. Kim, H. Y. Kim, and D. R. Lee, "Ruthenium doped TiO₂ fibers by electrospinning," *Inorganic Chemistry Communications*, vol. 7, no. 5, pp. 679–682, 2004.
- [3] Y. Xiaodan, W. Qingyin, J. Shicheng, and G. Yihang, "Nanoscale ZnS/TiO₂ composites: preparation, characterization, and visible-light photocatalytic activity," *Materials Characterization*, vol. 57, no. 4-5, pp. 333–341, 2006.
- [4] X. Zhang, S. Xu, and G. Han, "Fabrication and photocatalytic activity of TiO₂ nanofiber membrane," *Materials Letters*, vol. 63, no. 21, pp. 1761–1763, 2009.
- [5] S. Madhugiri, B. Sun, P. G. Smirniotis, J. P. Ferraris, and K. J. Balkus Jr., "Electrospun mesoporous titanium dioxide fibers," *Microporous and Mesoporous Materials*, vol. 69, no. 1-2, pp. 77–83, 2004.
- [6] B. Xin, L. Jing, Z. Ren, B. Wang, and H. Fu, "Effects of simultaneously doped and deposited Ag on the photocatalytic activity and surface states of TiO₂," *Journal of Physical Chemistry B*, vol. 109, no. 7, pp. 2805–2809, 2005.
- [7] J. Y. Park, I. H. Lee, and G. N. Bea, "Optimization of the electrospinning conditions for preparation of nanofibers from polyvinylacetate (PVAc) in ethanol solvent," *Journal of Industrial and Engineering Chemistry*, vol. 14, no. 6, pp. 707–713, 2008.
- [8] J.-Y. Park and I.-H. Lee, "Characterization and morphology of prepared titanium dioxide nanofibers by electrospinning," *Journal of Nanoscience and Nanotechnology*, vol. 10, no. 5, pp. 3402–3405, 2010.
- [9] S. Ramakrishna, K. Fujihara, W. E. Teo, T. C. Lim, and M. Zuwe M, *An Introduction Electrospinning and Nanofibers*, World Scientific Publishing Company, Singapore, 2005.
- [10] B. Ding, H. Y. Kim, C. K. Kim, M. S. Khil, and S. J. Park, "Morphology and crystalline phase study of electrospun TiO₂-SiO₂ nanofibers," *Nanotechnology*, vol. 14, no. 5, pp. 532–537, 2003.
- [11] C. Pan, L. Dong, and Z.-Z. Gu, "Surface functionalization of electrospun TiO₂ nanofibers by Au sputter coating for photocatalytic applications," *International Journal of Applied Ceramic Technology*, vol. 7, no. 6, pp. 895–901, 2010.
- [12] E. T. Bender, P. Katta, G. G. Chase, and R. D. Ramsier, "Spectroscopic investigation of the composition of electrospun titania nanofibers," *Surface and Interface Analysis*, vol. 38, no. 9, pp. 1252–1256, 2006.
- [13] A. K. Alves, F. A. Berutti, F. J. Clemens, T. Graule, and C. P. Bergmann, "Photocatalytic activity of titania fibers obtained by electrospinning," *Materials Research Bulletin*, vol. 44, no. 2, pp. 312–317, 2009.
- [14] B. Ding, C. K. Kim, H. Y. Kim, M. K. Seo, and S. J. Park, "Titanium dioxide nanofibers prepared by using electrospinning method," *Fibers and Polymers*, vol. 5, no. 2, pp. 105–109, 2004.
- [15] B. Xin, L. Jing, Z. Ren, B. Wang, and H. Fu, "Effects of simultaneously doped and deposited Ag on the photocatalytic activity and surface states of TiO₂," *Journal of Physical Chemistry B*, vol. 109, no. 7, pp. 2805–2809, 2005.
- [16] J. C. Yang, Y. C. Kim, Y. G. Shul, C. H. Shin, and T. K. Lee, "Characterization of photoreduced Pt/TiO₂ and decomposition of dichloroacetic acid over photoreduced Pt/TiO₂ catalysts," *Applied Surface Science*, vol. 121-122, pp. 525–529, 1997.
- [17] C.-C. Chang, J.-Y. Chen, T.-L. Hsu, C.-K. Lin, and C.-C. Chan, "Photocatalytic properties of porous TiO₂/Ag thin films," *Thin Solid Films*, vol. 516, no. 8, pp. 1743–1747, 2008.
- [18] J. C. Colmenares, M. A. Aramendía, A. Marinas, J. M. Marinas, and F. J. Urbano, "Synthesis, characterization and photocatalytic activity of different metal-doped titania systems," *Applied Catalysis A*, vol. 306, pp. 120–127, 2006.
- [19] J. M. G. Amores, V. S. Escibano, and G. Busca, "Anatase crystal growth and phase transformation to rutile in high-area TiO₂,

- MoO₃-TiO₂ and other TiO₂-supported oxide catalytic systems," *Journal of Materials Chemistry*, vol. 5, no. 8, pp. 1245–1249, 1995.
- [20] J. M. G. Amores, V. S. Escribano, G. Busca, and V. Lorenzelli, "Solid-state and surface chemistry of CuO-TiO₂ (anatase) powders," *Journal of Materials Chemistry*, vol. 4, no. 6, pp. 965–971, 1994.
- [21] H. E. Chao, Y. U. Yun, H. U. Xingfang, and A. Larbot, "Effect of silver doping on the phase transformation and grain growth of sol-gel titania powder," *Journal of the European Ceramic Society*, vol. 23, no. 9, pp. 1457–1464, 2003.
- [22] B. D. Cullity and S. R. Stock, *Elements of X-Ray Diffraction*, Prentice Hall, Upper Saddle River, NJ, USA, 3rd edition, 2001.



Hindawi

Submit your manuscripts at
<http://www.hindawi.com>

